

1 The Global Satellite Precipitation Constellation: current status and future requirements

2

3 Chris Kidd^{1,2}

4 George Huffman²

5 Viviana Maggioni³

6 Philippe Chambon⁴

7 Riko Oki⁵

8

9 ¹ *Earth System Science Interdisciplinary Center, University of Maryland, College Park, MD.*

10 *USA*

11 ² *NASA/Goddard Space Flight Center, Greenbelt, MD. USA*

12 ³ *Sid and Reva Dewberry Department of Civil, Environmental, and Infrastructure*

13 *Engineering, George Mason University, Fairfax, VA, USA*

14 ⁴ *CNRM, Université de Toulouse, Météo-France, CNRS, Toulouse, France*

15 ⁵ *Earth Observation Research Center, Japan Aerospace Exploration Agency, Ibaraki, Japan.*

16

17 **Capsule**

18 A robust constellation of precipitation-capable satellite sensors is necessary to capture and
19 map the spatial and temporal variability of precipitation across the Earth's surface.

20

21 **Abstract**

22 To address the need to map precipitation on a global scale a collection of satellites carrying
23 passive microwave (PMW) radiometers has grown over the last 20 years to form a
24 constellation of about 10-12 sensors at any one time. Over the same period, a broad range of
25 science and user communities has become increasingly dependent on the precipitation
26 products provided by these sensors. The constellation presently consists of both conical and
27 cross-track scanning precipitation-capable multi-channel instruments, many of which are
28 beyond their operational and design lifetime but continue to operate through the cooperation
29 of the responsible agencies. The Group on Earth Observations and the Coordinating Group
30 for Meteorological Satellites (CGMS), among other groups, have raised the issue of how a
31 robust, future precipitation constellation should be constructed. The key issues of current and
32 future requirements for the mapping of global precipitation from satellite sensors can be
33 summarised as providing: 1) sufficiently fine spatial resolutions to capture precipitation-scale
34 systems and reduce the beam-filling effects of the observations; 2) a wide channel diversity
35 for each sensor to cover the range of precipitation types, characteristics and intensities
36 observed across the globe; 3) an observation interval that provides temporal sampling
37 commensurate with the variability of precipitation; and 4) precipitation radars and
38 radiometers in low inclination orbit to provide a consistent calibration source, as
39 demonstrated by the first two spaceborne radar/radiometer combinations on the Tropical
40 Rainfall Measuring Mission (TRMM) and Global Precipitation Measurement (GPM) mission
41 Core Observatory (CO). These issues are critical in determining the direction of future

42 constellation requirements, while preserving the continuity of the existing constellation
43 necessary for long-term climate-scale studies.

44

45 **1 Introduction**

46 Water is not only a fundamental element of the Earth system, but also vital to all life on
47 Earth. Consequently, the observation and measurement of precipitation (rainfall and
48 snowfall) on a global scale is crucial to our understanding of the Earth system while
49 impacting society across many levels (Kirschbaum et al. 2017; Skofronick-Jackson et al.
50 2017). Precipitation provides a direct link between the global cycles of energy and water
51 through constraining and enabling the exchange of energy (Trenberth et al. 2009) and is the
52 primary control of many natural hazards such as droughts and floods (Vicente-Serrano et al.
53 2010; Kundzewicz et al. 2014). However, the variability of precipitation makes it difficult to
54 fully capture the characteristics of precipitation (Sidebar 1). Conventional measurements
55 made by rain (and snow) gauges are generally representative of a very small area close to
56 each gauge (Kyriakidis et al. 2001; Lundquist et al. 2019). While surface-based weather
57 radar observations have limitations (Harrison et al. 2000; Ciach and Krajewski 1999), they
58 provide valuable spatial measurements over large areas, complementing the global coverage
59 provided by gauge data. Crucially, over the oceans few or no observations are available (or
60 possible) through conventional means (Kidd et al. 2017). Even fundamental questions, such
61 as addressing the amount and occurrence of precipitation, are generally limited to land
62 regions (e.g. Sun et al. 2006; Herold et al. 2015). Observations provided by satellite sensors
63 are therefore key in the measurement of precipitation on a global scale (e.g. Adler et al.
64 2003). Since no single satellite can possibly achieve this coverage alone, a stable and robust
65 constellation is critical for providing sufficient temporal sampling to capture the vagaries of
66 precipitation, particularly in surface-data sparse regions such as over the Poles or oceans, to
67 provide consistent global precipitation products to the user community (Huffman et al. 2007).
68 Furthermore, long-term climate studies into changes in precipitation across the Earth's
69 surface can only be achieved through maintaining such a constellation (Adler et al. 2017;
70 Levizzani et al. 2018).

71

72 **2 Conventional precipitation measurements**

73 **2.1 Gauge measurements**

74 The *de facto* measuring device for precipitation is the rain (snow) gauge, typically consisting
75 of a funnel and a collection vessel, but with a wide range of designs (Strangeways 2004;
76 Sevruk and Klemm 1989). The amount of water collected is usually measured daily, but less
77 often in more remote regions. Automatic recording of the rainfall is possible with, for
78 example, tipping bucket gauges which record the time/date that a known quantity of rainfall
79 tips a small bucket (Sevruk 2005). Gauges are however subject to errors and uncertainties in
80 their measurements (Ciach 2003; Villarini et al. 2008). The primary error of gauge
81 measurements results from turbulence around the gauge orifice (Duchon and Biddle 2010)
82 which may cause significant under-catch in light rain and/or strong winds (Kochendorfer et
83 al. 2017). Measuring snowfall is more problematic due to the lower fall speeds of snowflakes

84 (Thériault et al 2012), resulting in the use of ‘shields’ around snow gauges to reduce the wind
85 speed around the gauge orifice (Duchon and Essenberg 2001). Despite issues relating to their
86 accuracy, gauges remain the mainstay of conventional global precipitation measurements,
87 particularly when corrections are applied (Michelson 2004). Even so, their coverage across
88 the globe is extremely variable. Over land, some regions have what could be considered
89 adequate coverage, while other regions have none. Measurements over oceans are only
90 available from a few atoll or island locations and a very small number of moored or drifting
91 buoys. Overall, the global surface represented by gauge measurements is pitifully small (Kidd
92 et al. 2017).

93

94 2.2 Weather radar measurements

95 The technological development of weather radar systems has created an important source of
96 information on precipitation at local to regional scales (Whiton et al 1998a, 1998b). Unlike
97 the point-measurements of gauges, radars can provide frequent, 3-dimensional observations
98 of precipitation up to about 250 km from the radar location (Zhang et al. 2011; Zhang et al.
99 2016). However, radars rely upon several assumptions to convert the backscatter signal from
100 rain and/or snow to an equivalent rain intensity (Campos and Zawadzki 2000; Uijlenhoet
101 2001; Uijlenhoet et al 2003). To avoid surface clutter the radar beam is usually elevated
102 resulting in the altitude of the beam increasing with range, thereby no longer measuring
103 surface precipitation and making near-surface phase (rainfall vs snowfall) detection difficult
104 (Mimikou and Baltas 1996). Furthermore, quantitative radar measurements of precipitation
105 are usually calibrated against gauge data where available, and due to the expense of
106 installation, operation, and maintenance, weather radars tend to be clustered in developed
107 countries, while their data may not be freely available.

108

109 2.3 Emerging systems

110 Over the last few years, a number of new surface-based instruments and techniques have
111 shown merit for measuring precipitation and augmenting conventional measurements,
112 particularly in regions with few or no surface observations. Over the oceans precipitation data
113 are particularly scarce, being limited island-gauges, buoys, or ships, and are typically not be
114 representative of the open ocean precipitation. Estimating rainfall through the use of
115 underwater hydrophones is presented by Pumphrey et al. (1989), Medwin et al. (1992) and
116 Forster (1994). More recently Ma and Nystuen (2005) found an excellent agreement between
117 acoustic, gauge and TRMM satellite measurements, particular at higher rain rates. While very
118 promising, the expense for deployment and maintenance of such instrumentation is
119 significant, although the rewards are likely to be great. Over land, the attenuation of
120 microwave communication signals by rainfall has been studied since the late 1960’s (see
121 Semplak and Turrin 1969). This path attenuation can now be fully exploited due to the
122 current widespread mobile phone infrastructure, as exemplified by the work by Leijnse et al.
123 (2007) over The Netherlands. Since the microwave paths are close to the surface, they tend to
124 be more representative of surface rainfall than weather radars. A more comprehensive study
125 by Overeem et al. (2011) showed very good correlations between the link-derived estimates

126 and those from the weather radar. Further development would complement and augment
127 existing precipitation measurements in regions where few precipitation observations exist.

128

129 **3 Satellite Precipitation Measurements**

130 3.1 Satellite systems and retrievals

131 Precipitation-capable satellites may be classified by their orbit and sensing frequencies. Low
132 Earth Orbiting (LEO) satellites orbit between 400-800 km altitude, provide about 14-16
133 orbits per day and typically operate in a Sun-synchronous orbit. Some low-inclination, non-
134 Sun-synchronous satellite orbits provide observations at different times of day as the orbits
135 precess over periods of weeks or months. The LEO satellites sensors generally provide a
136 broad sub-satellite swath of data, although some only provide data over a narrow swath or
137 only at nadir. The Cloud Profiling Radar (CPR) on CloudSat (Stephens et al. 2002; Stephens
138 et al. 2018), although not designed to retrieve precipitation, has shown significant merit in
139 observing and estimating light precipitation. Despite the nadir-only observations of the CPR,
140 its increased sensitivity has proved invaluable at providing an additional
141 calibration/validation data source for precipitation retrieval schemes, particularly for light
142 precipitation and snowfall (Battaglia et al. 2020). LEO satellites most relevant for
143 precipitation studies carry visible (VIS), Infrared (IR), passive microwave (PMW) and active
144 microwave (AMW) sensors (Kidd and Levizzani 2011). Geostationary (GEO) satellites
145 occupy a much higher orbit of about 35,800 km and are synchronised with the Earth's
146 rotation so appear stationary over a fixed location at the Equator, allowing frequent and
147 regular observations to be made. However, due to their altitude and requirements for
148 sufficiently fine-resolution measurements, these observations are currently restricted to
149 VIS/IR sensors. Mission concepts have been developed for geostationary PMW sensors (e.g.
150 Tanner et al. 2007; Lambrigtsen et al. 2007; Duruisseau et al. 2017; Lambrigsten 2019) but
151 these typically would only provide limited coverage at any one time and with limited
152 frequencies. Table 1 summarises the range of satellite observing systems.

153

154 Satellite observations for precipitation estimation extend back over 40 years, with the longest
155 data records based upon VIS and/or IR imagery. Early precipitation estimates relied upon
156 empirical relationships between the cloud top (brightness and/or temperature) characteristics
157 and surface rainfall (Kidd and Levizzani 2011). However, this relationship is generally poor
158 and inconsistent over time and space (Kidd and Muller 2010; Kidd and Levizzani 2019).
159 PMW radiometers, developed in the mid-1970s, rely upon the upwelling radiation from the
160 Earth's surface that is largely unaffected by the presence of cloud, particularly at the lower
161 frequencies (below 37 GHz). Sufficiently large liquid and ice particles (as in the case of
162 precipitation) affect the upwelling radiation, resulting in increased radiation at the lower
163 frequencies due to emission from liquid droplets, while at the higher frequencies ice particles
164 cause a decrease in the upwelling radiation (Kummerow 2020). Although PMW observations
165 are more direct than those of the VIS/IR, many assumptions are necessary to convert the
166 satellite observations into precipitation estimates, particularly over land, where low frequency
167 observations are impractical for retrieving precipitation. The most direct measure of

168 precipitation from space is obtained from precipitation radars and relies upon the backscatter
169 from the precipitation sized particles to estimate precipitation intensity in the same way as
170 their ground-based counterparts (see Battaglia et al. 2020). Two precipitation-specific radars
171 have flown; the first, the Tropical Rainfall Measuring Mission (TRMM) Precipitation Radar
172 (PR) operated at 13.6 GHz (Kummerow et al. 1998) and the Global Precipitation
173 Measurement (GPM) mission Dual-frequency Precipitation Radar (DPR) operating at 13.6
174 and 35.5 GHz (Hou et al. 2014), while the cloud-orientated CPR operates at 94 GHz. As with
175 ground-based radars, the backscatter-to-precipitation relationship is not consistent, and they
176 cannot retrieve precipitation within about 500-2000m of the surface due to clutter
177 (Skofronick-Jackson et al. 2019).

178

179 On a global scale the satellite-based observations largely address the shortcomings of
180 conventional measurements for observing precipitation while also providing data for studying
181 the characteristics and mechanisms of precipitation (Tapiador et al. 2011). However, to
182 measure and map precipitation correctly, satellite systems must provide sufficient sampling to
183 capture the temporal and spatial variability of precipitation.

184

185 3.2 Current precipitation constellation

186 The evolution of the constellation of precipitation-capable sensors is shown in Figure 1.
187 Conically-scanning PMW sensors began in the late 1980's, with cross-track scanning PMW
188 sounding instruments from the late 1990's onwards. The latter, although primarily designed
189 for retrieving temperature and humidity (Mo 1995), have proved valuable in increasing the
190 temporal sampling necessary for precipitation measurements (Kidd et al. 2016, 2021;
191 Bagaglini et al. 2021). The launch of TRMM (Simpson et al. 1988; Kummerow et al. 1998)
192 in 1997 facilitated multi-sensor retrievals through the inter-calibration of the then-available
193 PMW sensors with the TRMM instruments. This inter-calibration concept was expanded with
194 GPM (Hou et al. 2014; Skofronick-Jackson et al. 2017), launched in 2014.

195

196 The GPM-CO carries the DPR and the GPM Microwave Imager (GMI), both of which have
197 been shown to be very well calibrated (Wentz and Draper 2016). Alongside the GPM-CO, a
198 constellation of about 10-12 PMW-based precipitation-capable satellites is provided by
199 several international agencies (see Table 2). Amongst these are the operational missions of
200 NOAA (with the MHS and ATMS sensors), those of EUMETSAT (MetOp MHS) and the
201 U.S. Department of Defense (DoD) SSMIS sensors (Kidd et al. 2020). In addition, JAXA
202 contributes the AMSR-2, while the Centre National d'Etudes Spatiales (CNES) and the
203 Indian Space Research Organisation (ISRO) contribute SAPHIR from the Megha-Tropiques
204 mission (Roca et al 2015). Data archives of the observations from all of these and previous
205 PMW missions provide the necessary input for routine global estimates throughout the entire
206 record. Additional operational precipitation capable PMW missions exist (e.g. Li et al. 2018),
207 but due to data access/usage arrangements these cannot yet be fully exploited by the wider
208 precipitation community. The multi-agency co-ordination of the orbital crossing times of
209 these missions affects the temporal sampling. For example, at present the EUMETSAT,

210 NOAA and JAXA missions generally use station-keeping to ensure consistent overpass
211 times, while the crossing times of other PMW satellites drift over the course of 14-15 years
212 between the extremes of ca.13:30 to 22:30 (ascending node). A number of missions (i.e.
213 TRMM, GPM and Megha-Tropiques) had, or have, non-sun-synchronous precessing orbits
214 and therefore observe the full diurnal cycle at any one location over the period of a few
215 months, albeit with highly intermittent sampling (Roca et al. 2018).

216

217 In addition to the PMW sensors, a ring of GEO satellites provides frequent and regular vis/IR
218 observations (see Table 3) that are used to augment the LEO PMW observations. These
219 satellites' IR data are used as input for the NOAA Climate Precipitation Center (CPC) 4 km
220 30-minute global IR composite (Janowiak et al. 2001) and the GridSat collection at 10 km 3-
221 hour subsampled data (Knapp and Wilkins 2018) that are often used for precipitation
222 retrievals in conjunction with the LEO PMW observations. Merged PMW and IR satellite
223 schemes such as the CMORPH (Joyce and Xie 2011), GSMaP (Kubota et al 2020) and
224 IMERG (Huffman et al. 2020) allow precipitation products to be generated at resolutions of
225 30-minutes/10-km or better, which critically relies upon sufficient high-quality PMW
226 instantaneous retrievals of precipitation.

227

228 One of the pressing issues of the current constellation is the age of the satellite missions. It is
229 fortuitous that many of the precipitation-capable missions have lasted beyond their designed
230 operational lifetime with their respective agencies providing support to keep them operating.
231 However, before 2016 the mean age of these satellites was 5-7 years; after 2016 the age has
232 slowly risen and now is over 9 years (see Figure 2). Crucially, satellites fail and sensors fail,
233 often unexpectedly. A practical consequence of the gains and losses of these sensors is the
234 direct impact upon the temporal sampling by the constellation. For example, a failure of the
235 three oldest sensors in the constellation (the SSMISs on the DMSP F16 and F17 and the
236 SAPHIR on Megha-Tropiques) would lead to a loss in the temporal sampling, extending the
237 gaps between successive PMW observations, including the critical longest gaps, as illustrated
238 in Figure 3. A concerted program of new satellites/sensors is therefore necessary to ensure
239 the adequate continuation of precipitation measurements in a controlled and planned manner
240 to support the user requirements discussed below.

241

242 3.3 Planned precipitation-capable missions

243 Going forward, there are several planned satellite missions that are capable of providing
244 observations from which precipitation may be retrieved(see Figure 1). The precipitation-
245 capable missions planned for launch over the next decade include:

246

247 EUMETSAT: The European Polar-orbiting System (EPS) Second Generation (SG) will
248 provide continuity to the current MetOp series of satellites, and so the orbital characteristics
249 are likely to be commensurate with the current missions, including station keeping (Accadia
250 et al. 2020). The SG-A satellites will carry the cross-track MicroWave Sounder (MWS; 24
251 bands, 23-229 GHz, 40-17 km resolution), while the SG-B satellites will carry the conically

252 scanning MicroWave Imager (MWI; 18-bands, 18.7-183 GHz, 50-10 km resolution; Accadia
253 et al. 2020) and the Ice Cloud Imager (ICI; 11 bands, 183-664 GHz, 16 km resolution;
254 Eriksson et al. 2020). The SG-A and SG-B satellites are likely to be in the same orbital plane
255 but ½ orbit offset allowing adjacent swath coverage. Precise launch dates are yet to be
256 determined, but likely to be begin in the 2022/2023 timeframe.

257

258 NOAA: Additional members of the current Joint Polar System Satellite (JPSS) series (JPSS-
259 2/-3/-4) through the 2030's are likely to occupy the same orbit as NPP and NOAA-20
260 (Goldberg et al. 2013). Each will carry the ATMS sensor (22 band, 23-183 GHz), with
261 resolutions on the order of 16 km at nadir for the higher frequency channels, although the
262 resolution at 88.2 GHz channel is 32 km.

263

264 US Department of Defense: The DoD has a long history of precipitation-capable missions
265 (SSM/I and SSM/I), and DoD has commissioned Ball Aerospace to build a new PMW imager:
266 the Weather Satellite Follow-on – Microwave (WSF-M) (see Newell et al. 2020). The
267 planned sensor is a 6 frequency, 17 channel radiometer covering frequencies between 10-89
268 GHz with a finest spatial resolution of 15x10 km. The contractual launch date is set as
269 October 2023.

270

271 JAXA: The third generation of the Advanced Microwave Scanning Radiometer (AMSR-3)
272 sensor (Kasahara et al. 2020) is being built for installation on JAXA's Global Observation
273 SATellite for Greenhouse gases and Water cycle (GOSAT-GW) with a scheduled launch date
274 in 2023. The AMSR-3 sensor provides similar channel selection as the other AMSR sensors
275 (12-channel, 6.7-89 GHz), but with additional higher-frequency channels at 166 and 183
276 GHz.

277

278 NASA: Time-Resolved Observation of Precipitation structure and storm Intensity with a
279 Constellation of small Satellites (TROPICS) is a NASA Earth Venture Mission, providing 6
280 (plus one pathfinder) cubesats, primarily focused on the evolution of weather systems across
281 the Tropics (Blackwell et al. 2018). Each cubesat carries a small microwave radiometer
282 operating at frequencies between 90 and 204 GHz with spatial resolutions similar to the
283 MHS/ATMS sensors, and thus should be capable of providing observations for precipitation
284 retrievals. An initial pathfinder mission is scheduled for launch in June 2021.

285

286 Chinese Meteorological Agency (CMA): The FY series of satellites carrying the MWHS-2
287 and the MWRI instruments (Guo et al. 2015; Lawrence et al. 2018) has a proven record of
288 precipitation-capable missions. The planned Chinese Rain Mapping missions (FY-3I and FY-
289 3J) are expected to have capabilities similar to the GPM core observatory, hosting the PMW
290 MWRI/MWHS-2 sensors and a rain radar providing observations at 13.6 and 35.5 GHz, and
291 are currently planned to launch in 2022/2023.

292

293 Other missions of interest being developed include the European Copernicus Imaging
294 Microwave Radiometer (CIMR; Accadia et al. 2020), the ESA Arctic Weather Satellite
295 (AWS) and EarthCARE, and the NASA-led Aerosols, Clouds, Convection, Precipitation
296 mission (ACCP), which should be available for launch within the next decade. The Russian
297 Meteor-N series also host both PMW imagers and sounders although with limited dataaccess.
298 Many other small satellite missions (cubesats and smallsats) are proposed that could provide
299 precipitation-relevant data (see Stephens et al. 2020). However, it is vital that such
300 innovations support the spatial, temporal, channel, and quality requirements to address the
301 needs of the user community, as well as facilitate the integration of their observations into the
302 near real-time production of satellite precipitation products.

303

304 **4 Defining future mission requirements**

305 4.1 User requirements

306 The main drivers for all new missions are a necessary compromise between the requirements
307 of the user communities, the engineering/physical constraints, and the available budget. For
308 precipitation, the temporal and spatial resolutions for the observations (and hence derived
309 products) is determined by the capabilities of the observing system and the needs of the user
310 communities and their applications. Polls of the user community found significant variations
311 in the requirements of temporal and spatial sampling, as well as the latency (observation-to-
312 delivery delay) (see Table 4 and Figure 2, Friedl 2014) that depend on a huge range of
313 research and application topics. Perhaps the most stringent requirements were associated with
314 emergency managers, who require good spatial resolution (20 km or better), frequent (every
315 few minutes) and immediate (within a few minutes) information. For comparison, products
316 from the current constellation using combined PMW and IR observations provide products at
317 ca. 10 km resolution, every 30 minutes, within about 4 hours, although very near real time
318 IR-only products are available with reduced veracity. Importantly, the requirements within
319 each user community are very diverse, and moreover, the scales may vary within a particular
320 application, as demonstrated by Reed et al. (2015), who investigated the temporal sampling
321 of precipitation datasets for hydrological modelling to meet the necessary flood-forecasting
322 requirements. In that study, catchments with fast(slow) run-off characteristics require
323 information more(less) frequently. Consequently, it is important to address the most stringent
324 requirements as these are often those which have the greatest impact on both the physical and
325 human environment, although in reality, the available scales and sampling are often coarser
326 than the physical scales of precipitation and are further constrained by the physics and
327 engineering of the sensors.

328

329 4.2 Addressing the temporal sampling and spatial resolution.

330 *4.2.1 Spatial resolution at microwave frequencies* is essentially limited by the size of the
331 antenna (dish) that can be deployed, which is driven by current-generation engineering,
332 launch vehicle and budget limitations. For a given antenna size, the best available resolution
333 is inversely related to the observation frequency, meaning high-frequency channels have finer
334 resolution than low-frequency channels for the same sized antenna. At present, the finest

335 PMW resolution is about 3x5 km at 89, 166, and 183 GHz using a 2 m dish (e.g. the GMI).
336 Utilization of a larger dish is extremely problematic, both in terms of launch, and in terms of
337 operation since the dish is continually rotating. Deployments of large (5-6m) mesh antennas
338 are planned, such as the CIMR mission (Accadia et al. 2020), but are limited to the lower
339 frequency channels (<37 GHz) by the current-generation limits to dish surface conformance.
340 While GEO-based Synthetic Aperture systems have been studied for precipitation missions
341 (e.g. Lambrigsten 2019), they require significant additional processing, are not truly global
342 and envisage having only high frequency channels. Thus they presently do not necessarily
343 provide significant advantage over LEO-based radiometers. Since the spatial variability of
344 precipitation is on the order of a few km, resolving this variability at 1 km or less would be
345 ideal for satisfying the more-stringent user needs, and remains a significant and unmet
346 challenge.

347

348 *4.2.2 Temporal sampling from LEO satellites* is constrained not only by the physical number
349 of satellite sensors, but also by the swath over which each sensor collects data. For example,
350 the AMSR2 sensor (Imaoka et al. 2010) collects data across a 1450 km swath, while the GMI
351 has a swath of 885 km. Temporal sampling of 3 hours is often quoted as a minimum
352 requirement. This was originally based upon the number of samples necessary to reduce
353 ambiguities when observing the diurnal cycle of precipitation (by providing at least the first
354 three sinusoidal components), as well as being inherited from intermediate and Synoptic
355 hours (00 UTC, 03 UTC, etc), which has been the basis for the WMO-agreed distribution of
356 near-real-time GEO IR imagery. However, 3-hourly observations cannot adequately capture
357 the true precipitation accumulation at the daily scale, as illustrated in Figure 4. At 1 km an
358 accumulation of the 3-hourly sampled data attains a correlation of less than 0.5 against the
359 daily precipitation total and, while coarser resolutions provide higher correlations, even at 25
360 km resolution this does not exceed 0.8. This issue is further emphasised in Figure 5, which
361 shows the correlation of instantaneous PMW and IR estimates of precipitation against surface
362 radar over the course of 1 day (25 July 2015) over the central UK. Each peak in the
363 correlation represents the retrieval at a PMW sensor overpass. While the correlations between
364 the satellite and surface radar products are good across all the satellites at the time of
365 overpass, the correlation (in common with other measures) quickly deteriorates at times away
366 from the time of the overpass. Even when the IR data are directly calibrated with the surface
367 radar, as is done for Figure 5, the PMW products are much better. Despite a reasonable
368 number of PMW overpasses being available (as is currently the situation), there are clear
369 gaps (around 05:00 and 23:00 UTC) on this day where no PMW overpasses occur and
370 satellite precipitation estimates typically have to rely more heavily upon IR data.

371

372 **5 Strategies for maintaining a robust constellation**

373 The current precipitation constellation provides a significant number of observations to
374 generate precipitation estimates, but the continuity of these observations is very precarious.
375 Historically, the precipitation community has become very adept at collecting observations
376 from a diverse range of satellite missions and sensors, often not originally designed for the

377 retrieval of precipitation, as well as incorporating information from other water-related
378 missions to help close the water-cycle loop (Brocca et al. 2014; Behrangi 2020), but there is
379 presently no adequate substitute for a steady supply of precipitation-relevant observations. To
380 ensure a continuation of precipitation measurements from satellite systems, a number of
381 strategies need to be considered.

382

383 5.1 Maintaining/strengthening the constellation through new missions

384 This is undoubtedly the largest driver for maintaining the capabilities of the precipitation
385 constellation. The current constellation is continuously aging, with many of the current
386 sensors now more than 10 years old, well beyond their anticipated mission lifetime (see
387 Figure 2). Given the length of time required to design, build, test and launch new sensors it is
388 imperative that a long-term strategy for the constellation be devised and implemented. As
389 discussed in Section 3.3, several operational missions are planned, such as the NOAA JPSS
390 series, and the EUMETSAT EPS-SG series, but there are fewer dedicated long-term
391 precipitation-specific missions with mapping capabilities. While many operational missions
392 provide valuable observations for the precipitation community, such satellite sensors are not
393 necessarily optimised for precipitation retrievals, nor do the orbital characteristics provide the
394 frequent or uniform sampling necessary to capture the variability of precipitation. Observing
395 System Simulation Experiments (OSSE) could be used (e.g. Chambon et al. 2014) to improve
396 coordination between the satellite agencies is necessary to provide an optimal sampling
397 strategy. Studies have been undertaken to assess the likely impact of the loss of one or more
398 sensors within the constellation (Chambon et al. 2012).

399

400 5.2 Robustness through redundancy

401 Larger satellites are generally more robust at dealing with failures due to built-in redundancy,
402 allowing multi-decadal records of observations to be collected, as in the case of TRMM. The
403 long-term reliability of precipitation-capable cubesats and smallsats has yet to be fully
404 evaluated, but it is anticipated that the orbital characteristics would determine the mission
405 lifetime rather than system failure. Many operational meteorological satellites, such as the
406 GEO missions (GOES, Meteosat, etc.) and the MetOp and NOAA polar-orbiting missions
407 have on-orbit backup sensors. However, when the backup satellites continue to collect data
408 while the primary satellite is functioning, they generally do so over the same space/time
409 domains of the primary missions and therefore contribute relatively modestly to the overall
410 temporal sampling.

411

412 5.3 Extended mission lifetimes

413 Allowing missions to continue past their design lives and to continue contributing to the
414 precipitation constellation is a proven concept. However, the extension of missions is often
415 fraught with obstacles, not least being the need to comply with the modern standards for end-
416 of-life disposal of satellites to avoid space junk (Crowther 2002; Witze 2018). On a positive
417 note, the precipitation community has, in part, been successful in persuading agencies to keep
418 such missions operating after the end of their designed lifetime (e.g. TRMM), with partial

419 failures (e.g. Megha-Tropiques), or after station-keeping fuel was exhausted (e.g. MetOp-A).
420 The extension of mission lifetimes has only been, and likely will be, an issue for the larger
421 satellite systems.

422

423 5.4 Retrieval scheme resilience

424 Many current retrieval schemes require a full set of observations to generate a precipitation
425 estimate. However, many schemes could still contribute useful information with fewer
426 channels. Figure 6 shows a range of retrieval scenarios using different channel combinations.
427 The loss of a single channel on a diverse-channel sensor, such as the GMI, only degrades the
428 retrieved precipitation marginally. The better performance of precipitation retrievals from the
429 observations gathered over a wide range of frequencies has been shown by Kidd et al. (2018).
430 Additionally, the flexible utilisation of channels in the retrievals has particular merit when
431 dealing with surface-based Radio-Frequency Interference (RFI; Wu and Weng 2011), which
432 necessitates the exclusion of certain channels from retrieval schemes at certain
433 times/locations. Furthermore, the calculation of the errors and uncertainties associated with
434 the retrieved precipitation is urgently needed to allow users to assess the usefulness of
435 different retrievals. New techniques should also be investigated and developed that merge
436 observational data before the retrieval stage, rather than merging precipitation estimates post-
437 retrieval. The last point might be a longer-term goal, but it is possible to envisage a scenario
438 where two satellites in very similar orbits, both experiencing channel degradation could
439 jointly provide the capabilities of a single sensor.

440

441 5.5 Data availability and access

442 While most precipitation-related satellite observations are freely available both in terms of
443 being available and accessible to any particular user, and for that user to share more widely,
444 there are many data sets that are more restrictive and may not be accessible to all potential
445 users. Furthermore, the access to such data sets in very near real time is of great importance
446 to many user applications, such as flood forecasting, to ensure timely integration into their
447 processing systems. Crucially, science works best when such data are accessible to the
448 community, as shown by the open release of the DMSP SSMI data in 1987 by the US
449 Department of Defense, which enabled the careers many of the current generation of
450 precipitation scientists and the development of their retrieval schemes.

451

452 **6 Recommendations**

453 Based upon the current precipitation constellation and planned missions, the following course
454 of action is necessary to ensure the long-term continuity of global satellite precipitation
455 observations:

- 456 i) reaffirm commitment and support for current and planned precipitation-capable missions
457 with free and open data sharing by the appropriate agencies and organisations;
- 458 ii) develop a long-term strategy for a viable constellation of precipitation-capable sensors
459 that meet the necessary scientific and user requirements. Specifically,

- 460 a) PMW sensors with diverse channels covering the primary precipitation-sensitive
461 frequencies with good spatial resolution as exemplified by the AMSR/GMI class of
462 sensors, and
463 b) operational AMW sensors in a non-Sun-synchronous orbit for cross-calibration and
464 reference standard for PMW (and IR) precipitation estimates, as exemplified by the
465 mapping capabilities of the PR/DPR and the sensitivity of the CPR;
466 iii) support the continuation of precipitation-capable missions beyond nominal mission
467 lifetime operations, with due regard for the limitations imposed by deorbiting/sensor
468 degradation considerations;
469 iv) integrate new technologies, such as smallsats and cubesats, with access to new data sets
470 where these address the necessary scientific and user requirements; and
471 v) implement mitigation strategies within the precipitation retrieval schemes to maximise
472 use of sub-optimal observations, including failed/denied channels, to help ensure
473 continuity in adequate sampling.

474

475 **Acknowledgements:**

476 The Authors acknowledge the formative role in this work that was provided by many
477 colleagues' discussions, presentations, and working group deliberations in the International
478 Precipitation Working Group, the Precipitation Virtual Constellation working group of the
479 Committee on Earth Observation Satellites, the Integrated Global Water Cycle Observations
480 community of practice, and many specialty conference sessions. Funding for Kidd is in part
481 from the NASA/GSFC-UMD/ESSIC cooperative agreement, NASA grant NNX17AE79A.

482

483 **References:**

- 484 Accadia, C., V. Mattioli, P. Colucci, P. Schlüssel, S. D'Addio, U. Klein, T. Wehr, and C.
485 Donlon, 2020: Microwave and submm wave sensors: A European perspective. In: Satellite
486 Precipitation Measurement, V. Levizzani, C. Kidd., D. B. Kirschbaum, C. D. Kummerow, K.
487 Nakamura, F. J. Turk, Eds., Springer Nature, Cham, *Advances in Global Change Research*,
488 **67**, 83-97, https://doi.org/10.1007/978-3-030-24568-9_5.
- 489 Adler, R. F., and Coauthors, 2003: The Version-2 Global Precipitation Climatology Project
490 (GPCP) Monthly Precipitation Analysis (1979–Present). *J. Hydrometeor.*, **4**, 1147–1167,
491 [https://doi.org/10.1175/1525-7541\(2003\)004<1147:TVGPCP>2.0.CO;2](https://doi.org/10.1175/1525-7541(2003)004<1147:TVGPCP>2.0.CO;2).
- 492 Adler, R. F., G. Gu, M. Sapiano, J. J. Wang, and G. J. Huffman, 2017: Global precipitation:
493 Means, variations and trends during the satellite era (1979–2014). *Surveys in Geophysics*, **38**,
494 **4**, 679-699, <https://doi.org/10.1007/s10712-017-9416-4>
- 495 Bagaglini, L. Sanò, P., Casella, D., Cattani, E., Panegrossi, G. 2021 The Passive microwave
496 Neural network Precipitation Retrieval algorithm for climate applications (PNPR-CLIM):
497 design and application. *Remote Sens.* **13**, 1701. <https://doi.org/10.3390/rs13091701> Battaglia,
498 A., Kollias, P., Dhillon, R., Roy, R., Tanelli, S., Lamer, K., Grecu, M., Lebsock, M., Watters,
499 D., Mroz, K., Heymsfield, G., Li, L. H., Furukawa, K. 2020: Space-borne cloud and
500 precipitation radars: status, challenges and ways forward. *Reviews of Geophysics*, **58**, **3**,
501 e2019RG000686. <https://doi.org/10.1029/2019RG000686>
- 502 Behrangi, A., 2020: Improving High-latitude and cold region precipitation analysis. In:
503 Satellite Precipitation Measurement, V. Levizzani, C. Kidd., D. B. Kirschbaum, C. D.
504 Kummerow, K. Nakamura, F. J. Turk, Eds., Springer Nature, Cham, Advances in Global

505 [Change Research](https://doi.org/10.1007/978-3-030-35798-6_21), **69**, 881-895, https://doi.org/10.1007/978-3-030-35798-6_21. Bizzarri, B.,
506 Amato, U., Bates, J., Benesch, W., Bühler, S., Capaldo, M., Cervino, M., Cuomo, V., De
507 Leonibus, L., Desbois, M., et al. 2002: Requirements and perspectives for MW/sub-mm
508 sounding from geostationary satellite. In Proceedings of the EUMETSAT Meteorological
509 Satellite Conference, Dublin, Ireland, 2–6 September 2002; pp. 97–105.

510 Blackwell, W. J., S. Braun, R. Bennartz, C. Velden, M. DeMaria, R. Atlas, J. Dunion, F.
511 Marks, R. Rogers, B. Annane, and R. V. Leslie, 2018: An overview of the TROPICS NASA
512 Earth Venture Mission. *Advances in Remote Sensing of Rainfall and Snowfall* **144**, S1, 16-26.
513 <https://doi.org/10.1002/qj.3290>

514 Brocca, L., Ciabatta, L., Massari, C., Moramarco, T., Hahn, S., Hasenauer, S., Kidd, R.,
515 Dorigo, W., Wagner, W., Levizzani, V., 2014: Soil as a natural rain gauge: Estimating global
516 rainfall from satellite soil moisture data. *Journal of Geophysical Research: Atmospheres* **119**,
517 5128–5141. <https://doi.org/10.1002/2014JD021489>

518 Campos, E., and I. Zawadzki, 2000: Instrumental Uncertainties in Z–R Relations. *J. Appl.*
519 *Meteor.*, **39**, 1088–1102, [https://doi.org/10.1175/1520-](https://doi.org/10.1175/1520-0450(2000)039<1088:IUIZRR>2.0.CO;2)
520 [0450\(2000\)039<1088:IUIZRR>2.0.CO;2](https://doi.org/10.1175/1520-0450(2000)039<1088:IUIZRR>2.0.CO;2).

521 Chambon, P., Roca, R., Jobard, I., & Capderou, M. 2012: The sensitivity of tropical rainfall
522 estimation from satellite to the configuration of the microwave imager constellation. *IEEE*
523 *Geoscience and Remote Sensing Letters*, **10**, 996-1000.
524 <https://doi.org/10.1109/LGRS.2012.2227668>

525 Chambon, P., Zhang, S.Q., Hou, A.Y., Zupanski, M. and Cheung, S. 2014: Assessing the
526 impact of pre-GPM microwave precipitation observations in the Goddard WRF ensemble
527 data assimilation system. *Quart. J. Roy. Meteorol. Soc.*, **140**, 1219-1235.
528 <https://doi.org/10.1002/qj.2215>

529 Ciach, G. J., and W. F. Krajewski, 1999: Radar–Rain Gauge Comparisons under
530 Observational Uncertainties. *J. Appl. Meteor.*, **38**, 1519–1525, [https://doi.org/10.1175/1520-](https://doi.org/10.1175/1520-0450(1999)038<1519:RRGCUO>2.0.CO;2)
531 [0450\(1999\)038<1519:RRGCUO>2.0.CO;2](https://doi.org/10.1175/1520-0450(1999)038<1519:RRGCUO>2.0.CO;2).

532 Ciach, G. J., 2003: Local Random Errors in Tipping-Bucket Rain Gauge Measurements. *J.*
533 *Atmos. Oceanic Technol.*, **20**, 752–759, [https://doi.org/10.1175/1520-](https://doi.org/10.1175/1520-0426(2003)20<752:LREITB>2.0.CO;2)
534 [0426\(2003\)20<752:LREITB>2.0.CO;2](https://doi.org/10.1175/1520-0426(2003)20<752:LREITB>2.0.CO;2).

535 Crowther, R., 2002: Space Junk--Protecting Space for Future Generations. *Science* **296**, 5571,
536 1241-1242. <https://doi.org/10.1126/science.1069725>

537 Duchon, C. E., and G. R. Essenberg, 2001: Comparative rainfall observations from pit and
538 aboveground rain gauges with and without wind shields, *Water Resour. Res.*, **37**, 12, 3253–
539 3263, <https://doi.org/10.1029/2001WR000541>.

540 Duchon, C. E., and C. J. Biddle, 2010: Undercatch of tipping-bucket gauges in high rain rate
541 events. *Adv. Geosci.* **25**, 11–15, <https://doi.org/10.5194/adgeo-25-11-2010>.

542 Duruisseau, F., Chambon, P., Guedj, S., Guidard, V., Fourrié, N., Taillefer, F., Brousseau, P.,
543 Mahfouf, J.-F. and Roca, R., 2017: Investigating the potential benefit to a mesoscale NWP
544 model of a microwave sounder on board a geostationary satellite. *Quart. J. Roy. Meteorol.*
545 *Soc.*, **143**: 2104-2115. <https://doi.org/10.1002/qj.3070>

546 Eriksson, P., B. Rydberg, V. Mattioli, A. Thoss, C. Accadia, U. Klein, and S. Buehler, 2020:
547 Towards an operational Ice Cloud Imager (ICI) retrieval product, *Atmos. Meas. Tech.*, **13**,
548 53–71, <https://doi.org/10.5194/amt-13-53-2020>

549 Forster, J., 1994: Rain measurement on buoys using hydrophones. *IEEE Journal of Oceanic*
550 *Engineering*, **19**, 1, 23-29, <https://doi.org/10.1109/48.289446>.

551 Friedl, L., 2014: GEO Task US-09-01a: Critical Earth observation priorities; Precipitation
552 data characteristics and user types, pp. 60 (Available at
553 https://sbageotask.larc.nasa.gov/Weather_US0901a-FINAL.pdf)

554 Goldberg, M. D., H. Kilcoyne, H. Cikanek, and A. Mehta, 2013: Joint Polar Satellite System:
555 The United States next generation civilian polar-orbiting environmental satellite system,
556 *Journal of Geophysical Research-Atmospheres* **118**, 24, 13463-13475.
557 <https://doi.org/10.1002/2013JD020389>

558 Guo, Y., N. M. Lu, C. L. Qi, S. Y. Gu, and J. M. Xu, 2015: Calibration and validation of
559 microwave humidity and temperature sounder onboard FY-3C satellite. *Chinese Journal of*
560 *Geophysics-Chinese Edition* **58**, 1, 20-31, <https://doi.org/10.6038/cjg20150103>

561 Harrison, D. L., S. J. Driscoll, and M. Kitchen, 2000: Improving precipitation estimates from
562 weather radar using quality control and correction techniques, *Meteor. Apps.* **7**, 2, 135-144.
563 <https://doi.org/10.1017/S1350482700001468>

564 Herold, N., L. V. Alexander, M. G. Donat, S. Contractor, A. Becker, 2012: How much does it
565 rain over land? *Geophys. Res. Lett.* **43**:341–348, <https://doi.org/10.1002/2015GL066615>.

566 Hou, A.Y., R. K. Kakar, S. A. Neeck, A. Azarbarzin, C. D. Kummerow, M. Kojima, R. Oki,
567 K. Nakamura, T. Iguchi, 2014: The Global Precipitation Measurement mission. *Bull. Amer.*
568 *Meteor. Soc.* **95**, 701-722, <https://doi.org/10.1175/BAMS-D-13-00164.1>.

569 Huffman, G. J., and Coauthors, 2007: The TRMM Multisatellite Precipitation Analysis
570 (TMPA): Quasi-Global, Multiyear, Combined-Sensor Precipitation Estimates at Fine Scales.
571 *J. Hydrometeor.*, **8**, 38–55, <https://doi.org/10.1175/JHM560.1>.

572 Huffman, G. J., V. Levizzani, R. R. Ferraro, F. J. Turk, and C. Kidd, 2016: Requirements for
573 a robust precipitation constellation. *14th Specialist Meeting on Microwave Radiometry and*
574 *Remote Sensing of the Environment (MicroRad)*, Espoo, 2016, 37-41.

575 Huffman, G. J., and Coauthors, 2020: Integrated Multi-satellite Retrievals for the Global
576 Precipitation Measurement (GPM) Mission (IMERG). In: *Satellite Precipitation*
577 *Measurement*, V. Levizzani, C. Kidd., D. B. Kirschbaum, C. D. Kummerow, K. Nakamura,
578 F. J. Turk, Eds., Springer Nature, Cham, *Advances in Global Change Research*, **7**, 343-353,
579 https://doi.org/10.1007/978-3-030-24568-9_19.

580 Imaoka K., and Coauthors, 2010: "Global Change Observation Mission (GCOM) for
581 Monitoring Carbon, Water Cycles, and Climate Change," in *Proceedings of the IEEE*, **98**, 5,
582 717-734. <https://doi.org/10.1109/JPROC.2009.2036869>.

583 Janowiak, J. E., Joyce, R. J., & Yarosh, Y. (2001). A Real-Time Global Half-Hourly Pixel-
584 Resolution Infrared Dataset and Its Applications, *Bull. Amer. Meteor. Soc.*, **82**, 205-218.
585 [https://doi.org/10.1175/1520-0477\(2001\)082<0205:ARTGHH>2.3.CO;2](https://doi.org/10.1175/1520-0477(2001)082<0205:ARTGHH>2.3.CO;2)

586 Joyce, R. J., and P. Xie, 2011: Kalman Filter–Based CMORPH. *J. Hydrometeor.*, **12**, 1547–
587 1563, <https://doi.org/10.1175/JHM-D-11-022.1>.

588 Kasahara, M., M. Kachi, K. Inaoka, H. Fujii, T. Kubota, R. Shimada, and Y. Kojima, 2020:
589 Overview and current status of GOSAT-GW mission and AMSR3 instrument. *Proc. SPIE*
590 **11530**, Sensors, Systems, and Next-Generation Satellites XXIV, 1153007 (20 September
591 2020). <https://doi.org/10.1117/12.2573914>

592 Kidd, C., and C. Muller, 2010: The combined passive microwave-infrared (PMIR) algorithm.
593 *Satellite Rainfall Applications for Surface Hydrology*, F. Hossain and M. Gebremichael Ed.,
594 Dordrecht, 2010, pp 69-83, https://doi.org/10.1007/978-90-481-2915-7_5.

595 Kidd, C., and V. Levizzani, 2011: Status of satellite precipitation retrievals. *Hydrol. Earth*
596 *Syst. Sci.*, **15**, 1109-1116, <https://doi.org/10.5194/hess-15-1109-2011>

597 Kidd, C., T. Matsui, J. Chern, K. Mohr, C. Kummerow, and D. Randel, 2016: Global
598 Precipitation Estimates from cross-track passive microwave observations using a physically
599 based retrieval scheme. *J. Hydrometeor.*, **17**, 383-400, [https://doi.org/10.1175/JHM-D-15-](https://doi.org/10.1175/JHM-D-15-0051.1)
600 0051.1

601 Kidd, C., A. Becker, G. J. Huffman, C. L. Muller, P. Joe, G. Skofronick-Jackson, and D. B.
602 Kirschbaum, 2017: So, How Much of the Earth's Surface *Is* Covered by Rain Gauges? *Bull.*
603 *Amer. Meteor. Soc.*, **98**, 69–78, <https://doi.org/10.1175/BAMS-D-14-00283.1>.

604 Kidd, C., J. Tan, P-E. Kirstetter, and W. A. Petersen, 2018: Validation of the Version 05
605 Level 2 precipitation products from the GPM Core Observatory and constellation satellite
606 sensors. *Quart. J. Roy. Meteorol. Soc.*, **144**, 313– 328. <https://doi.org/10.1002/qj.3175>

607 Kidd, C., and V. Levizzani, 2019: Quantitative precipitation Estimation from Satellite
608 Observations. *Extreme Hydroclimatic Events and Multivariate Hazards in a Changing*
609 *Climate*, V. Maggioni and C. Massari, Ed., Elsevier, [https://doi.org/10.1016/B978-0-12-](https://doi.org/10.1016/B978-0-12-814899-0.00001-8)
610 814899-0.00001-8.

611 Kidd, C., Y.N. Takayabu, G. M. Skofronick-Jackson, G. J. Huffman, S. A. Braun, T. Kubota,
612 and F. J. Turk, 2020: The Global Precipitation Measurement (GPM) Mission. *Satellite*
613 *Precipitation Measurement*. V. Levizzani, C. Kidd, D. B. Kirschbaum, C. D. Kummerow, K.
614 Nakamura, and F. J. Turk, Ed., Springer Nature, 3-23, [https://doi.org/10.1007/978-3-030-](https://doi.org/10.1007/978-3-030-24568-9_1)
615 24568-9_1.

616 Kidd, C., Matsui, T., Ringerud, S. 2021: Precipitation Retrievals from Passive Microwave
617 Cross-Track Sensors: The Precipitation Retrieval and Profiling Scheme. *Remote Sens.* **13**,
618 947. <https://doi.org/10.3390/rs13050947>

619 Kirschbaum, D. B., and Coauthors, 2017: NASA's Remotely Sensed Precipitation: A
620 Reservoir for Applications Users. *Bull. Amer. Meteor. Soc.*, **98**, 1169–1184,
621 <https://doi.org/10.1175/BAMS-D-15-00296.1>.

622 Knapp, K. R., and S. L. Wilkins, 2018: Gridded satellite (GridSat) GOES and CONUS data.
623 *Earth Syst. Sci. Data*, **10**, 1417–1425, <https://doi.org/10.5194/essd-10-1417-2018>.

624 Kochendorfer, J., R. Rasmussen, M. Wolff, B. Baker, M.E. Hall, T. Meyers, S. Landolt, A.
625 Jachcik, K. Isaksen, R. Brækkan, and R. Leeper, 2017: The quantification and correction of
626 wind-induced precipitation measurement errors. *Hydrol. Earth Syst. Sci.*, **21**, 1973–1989,
627 <https://doi.org/10.5194/hess-21-1973-2017>

628 Kubota, T., K. Aonashi, T. Ushio, S. Shige, Y. N. Takayabu, M. Kachi, Y. Arai, T. Tashima,
629 T. Masaki, N. Kawamoto, T. Mega, M. K. Yamamoto, A. Hamada, M. Yamaji, G. Liu, and
630 R. Oki, 2020: Global Satellite Mapping of Precipitation (GSMaP) products in the GPM era.
631 *Satellite Precipitation Measurement*, V. Levizzani, C. Kidd., D. B. Kirschbaum, C. D.
632 Kummerow, K. Nakamura, F. J. Turk, Eds., Springer Nature, *Advances in Global Change*
633 *Research*, **67**, 355-373, https://doi.org/10.1007/978-3-030-24568-9_20.

634 Kummerow, C. D., W. Barnes, T. Kozu., J. Shiue, and J. Simpson, 1998: The Tropical
635 Rainfall Measuring Mission (TRMM) sensor package. *J. Atmos. Oceanic Technol.* **15**, 809-
636 817, [https://doi.org/10.1175/1520-0426\(1998\)015%3C0809:TTRMMT%3E2.0.CO;2](https://doi.org/10.1175/1520-0426(1998)015%3C0809:TTRMMT%3E2.0.CO;2), 1998.

637 Kummerow, C. D., 2020: Introduction to passive microwave retrieval methods. *Satellite*
638 *Precipitation Measurement*. V. Levizzani, C. Kidd, D. B. Kirschbaum, C. D. Kummerow, K.
639 Nakamura, and F. J. Turk, Eds., Springer Nature, 123-140, [https://doi.org/10.1007/978-3-](https://doi.org/10.1007/978-3-030-24568-9_7)
640 030-24568-9_7.

641 Kundzewicz, Z. W., and Coauthors, 2014: Flood risk and climate change: global and regional
642 perspectives. *Hydrological Sciences Journal – Journal Des Sciences Hydrologiques* **59**, 1-28.
643 <https://doi.org/10.1080/02626667.2013.857411>

644 Kyriakidis, P. C., J. Kim, and N. L. Miller, 2001: Geostatistical Mapping of Precipitation
645 from Rain Gauge Data Using Atmospheric and Terrain Characteristics. *J. Appl. Meteor.*, **40**,
646 1855–1877, [https://doi.org/10.1175/1520-0450\(2001\)040<1855:GMOPFR>2.0.CO;2](https://doi.org/10.1175/1520-0450(2001)040<1855:GMOPFR>2.0.CO;2).

647 Lambriksen, B.H., S.T. Brown, S.J. Dinardo, T.C. Gaier, P.P. Kangaslahti, and A.B.Tanner
648 2007: GeoSTAR—A geostationary microwave sounder for the future. Available at
649 <https://trs.jpl.nasa.gov/bitstream/handle/2014/41287/07-2264.pdf> Last accessed 02 March
650 2020.

651 Lambriksen, B, 2019: Observing clouds, convection and precipitation with a geostationary
652 microwave sounder. 2019 IEEE International Geoscience and Remote Sensing Symposium
653 (IGARSS 2019), JUL 28-AUG 02, 2019, Yokohama, JAPAN pp7548-7551.

654 Lawrence, H., N. Bormann, A. Geer, Q. Lu, and S. J. English, 2018: Evaluation and
655 Assimilation of the Microwave Sounder MWHS-2 Onboard FY-3C in the ECMWF
656 Numerical Weather Prediction System. *IEEE Transactions on Geoscience and Remote*
657 *Sensing* 56, 6, 3333-3349. <https://doi.org/10.1109/TGRS.2018.2798292>.

658 Leijnse, H., R. Uijlenhoet, and J. N. M. Stricker, 2007: Rainfall measurement using radio
659 links from cellular communication networks, *Water Resour. Res.*, **43**, W03201,
660 <https://doi.org/10.1029/2006WR005631>.

661 Levizzani V., Kidd, C., Aonashi, K., Bennartz, R., Ferraro, R.R., Huffman, G. J., Roca, R.,
662 Turk, F.J., Wang, N-Y. 2018: The activities of the International Precipitation Working
663 Group, *Quart. J. Roy. Meteorol. Soc.* 144, 3-15. doi:10.1002/qj.3214

664 Li N, J. He, S. Zhang, and N. Lu, 2018: Precipitation Retrieval Using 118.75-GHz and
665 183.31-GHz Channels from MWHS on FY-3C Satellite, in *IEEE Journal of Selected Topics*
666 *in Applied Earth Observations and Remote Sensing*, **11**, 4373-4389,
667 <https://doi.org/10.1109/JSTARS.2018.2873255>.

668 Luini, L., and C. Capsoni, C., 2012: The impact of space and time averaging on the spatial
669 correlation of rainfall, *Radio Sci.*, 47, RS3013, doi:10.1029/2011RS004915.

670 Lundquist, J., M. Hughes, E. Gutmann, and S. Kapnick, 2019: Our Skill in Modeling
671 Mountain Rain and Snow is Bypassing the Skill of Our Observational Networks. *Bull. Amer.*
672 *Meteor. Soc.*, **100**, 2473–2490, <https://doi.org/10.1175/BAMS-D-19-0001.1>.

673 Ma, B. B., and J.A. Nystuen, 2005: Passive Acoustic Detection and Measurement of Rainfall
674 at Sea, *J. Atmos. Oceanic Technol.*, 22, 1225-1248, <https://doi.org/10.1175/JTECH1773.1>

675 Medwin, H., J. A. Nystuen, P. W. Jacobus, L. H. Ostwald and D. E. Snyder, 1992: The
676 anatomy of underwater rain noise. *J. Acoust. Soc. Amer.*, **92**, 1613-1623,
677 <https://doi.org/10.1121/1.403902>

678 Michelson, D.B. 2004: Systematic correction of precipitation gauge observations using
679 analyzed meteorological variables. *J. Hydrology*, **290**, 3–4, 161-177. <https://doi.org/10.1016/j.jhydrol.2003.10.005>

681 Mimikou, M.A., and E. A. Baltas, 1996: Flood Forecasting Based on Radar Rainfall
682 Measurements. *J. Water Resources Planning and Management*, **122**, 3.
683 [https://doi.org/10.1061/\(ASCE\)0733-9496\(1996\)122:3\(151\)](https://doi.org/10.1061/(ASCE)0733-9496(1996)122:3(151))

684 Mo, T. 1995: A study of the microwave sounding unit on the NOAA-12 satellite. *IEEE*
685 *Transactions on Geoscience and Remote Sensing*, **33**, 1141–1152.
686 <https://doi.org/10.1109/36.469478>.

687 Newell, D., D. Draper, Q. Remund, B. Woods, C. Mays, B. Bensler, D. Miller, and K.
688 Eastman, 2020: Weather Satellite Follow-On – Microwave (WSF-M) Design And Predicted
689 Performance, AMS 20th Symposium on Meteorological Observation and Instrumentation,

690 Boston, MA, USA, 13-16 January 2020,
691 <https://ams.confex.com/ams/2020Annual/webprogram/Paper369912.html>

692 Overeem, A., H., Leijnse, and R. Uijlenhoet, 2011: Measuring urban rainfall using
693 microwave links from commercial cellular communication networks, *Water Resour. Res.*, **47**,
694 W12505, <https://doi.org/10.1029/2010WR010350>.

695 Pumphrey, H.C., L. A. Crum and L. Bjørnø, 1989: Underwater sound produced by individual
696 drop impacts and rainfall, *J. Acoust. Soc. Amer.*, **85**, 1518-1526.
697 <https://doi.org/10.1121/1.397353>

698 Reed, P. M., N. W. Chaney, J.D. Herman, M. P. Ferringer, and E. F. Wood, 2015:
699 Internationally coordinated multi-mission planning is now critical to Sustain the space-based
700 rainfall observations needed for managing floods globally. *Environ. Res. Lett.*, **10**, 7.
701 <https://doi.org/10.1088/1748-9326/10/2/024010>

702 Roca, R., Brogniez, H., Chambon, P., Chomette, O., Cloché, S., Gosset, M., Mahfouf, J.F.,
703 Raberanto, P. and Viltard, N. 2015: The Megha-Tropiques mission: a review after three years
704 in orbit. *Frontiers in Earth Science*, 3, 1-14. <https://doi.org/10.3389/feart.2015.00017>.

705 Roca, R., N. Taburet, E. Lorant, et al. 2018: Quantifying the contribution of the Megha-
706 Tropiques mission to the estimation of daily accumulated rainfall in the Tropics. *Quart. J*
707 *Roy. Meteor. Soc.* 144, 49– 63. <https://doi.org/10.1002/qj.3327>

708 Semplak, R. A., and R. H. Turrin, 1969: Some measurements of attenuation by rainfall at
709 18.5 GHz, *Bell Syst. Technol. J.*, 48, 1767– 1787. [https://doi.org/10.1002/j.1538-](https://doi.org/10.1002/j.1538-7305.1969.tb01151.x)
710 [7305.1969.tb01151.x](https://doi.org/10.1002/j.1538-7305.1969.tb01151.x)

711 Simpson, J. R., R. F. Adler, G. R. North, 1988: A proposed Tropical Rainfall Measuring
712 Mission (TRMM) satellite. *Bull. Amer. Meteor. Soc.* **69**, 278-295,
713 [https://doi.org/10.1175/1520-0477\(1988\)069,0278:APTRMM.2.0.CO;2](https://doi.org/10.1175/1520-0477(1988)069<0278:APTRMM.2.0.CO;2), 1988.

714 Skofronick-Jackson, G., and Coauthors, 2017: The Global Precipitation Measurement (GPM)
715 mission for science and society. *Bull. Amer. Meteor. Soc.* **98**, 1679–1695
716 <https://doi.org/10.1175/BAMS-D-15-00306.1>.

717 Skofronick-Jackson, G., M. Kulie, L. Milani, S. J. Munchak, N. B. Wood, and V. Levizzani,
718 2019: Satellite Estimation of Falling Snow: A Global Precipitation Measurement (GPM)
719 Core Observatory Perspective, *J. Appl. Meteor. Climatol.*, **58**, 1429-1448.
720 <https://doi.org/10.1175/JAMC-D-18-0124.1>

721 Sevruk B., and S. Klemm, 1989: *Catalogue of Standard Precipitation Gauges, Instruments*
722 *and observing methods*, Rep, vol. 39, World Meteorol. Org., WMO, Geneva (1989)
723 WMO/TD No. 328, 52 pp.

724 Sevruk, B., 2005: Rainfall measurement: gauges. *Encyclopedia of Hydrological Sciences,*
725 *Part 2, Hydrometeorology.* M.G. Anderson Ed., 40, 1, Wiley&Sons Ltd, Chichester, UK. 8
726 pp.

727 Stephens, G.L., and Coauthors, 2002: The CloudSat mission and the A-Train: A new
728 dimension of space-based observations of clouds and precipitation. *Bull. Amer. Meteor. Soc.*
729 **83**, 1771-1790, <https://doi.org/10.1175/BAMS-83-12-1771>.

730 Stephens, G., D. Winker, J. Pelon, C. Trepte, D. Vane, C. Yuhas, T. L'Ecuyer, and M.
731 Lebsock, 2018: *CloudSat* and *CALIPSO* within the A-Train: Ten Years of Actively
732 Observing the Earth System. *Bull. Amer. Meteor. Soc.*, **99**, 569–581,
733 <https://doi.org/10.1175/BAMS-D-16-0324.1>.

734 Stephens, G., Freeman, A., Richard, E., Pilewskie, P., Larkin, P., Chew, C., Tanelli, S.,
735 Brown, S., Posselt, D., Peral, E., 2020. The Emerging Technological Revolution in Earth

736 Observations. *Bulletin of the American Meteorological Society* 101, E274–E285.
737 <https://doi.org/10.1175/BAMS-D-19-0146.1>

738 Strangeways, I.C., 20014: Improving precipitation measurement. *Int. J. Climatol.* **24**, 1443–
739 1460, <https://doi.org/10.1002/joc.1075>.

740 Sun, Y., S. Solomon, A. Dai, and R. W. Portmann, 2006: How Often Does It Rain? *J.*
741 *Climate*, **19**, 916–934, <https://doi.org/10.1175/JCLI3672.1>.

742 Tanner, A. B., and Coauthors, 2007: Initial results of the Geostationary Synthetic Thinned
743 Array Radiometer. *IEEE Trans. Geosci. Remote Sens.*, **45**, 9.
744 <https://doi.org/10.1109/TGRS.2007.894060>

745 Tapiador, F. J., Turk, J., Petersen, W., Hou, A. Y., García-Ortega, E., Machado, L. A. T.,
746 Angelis, C. F., Salio, P., Kidd, C., Huffman, G. J., 2011: Global precipitation measurement:
747 Methods, datasets and applications. *Atmospheric Research* 104–105, 70–97.
748 <https://doi.org/10.1016/j.atmosres.2011.10.021>

749 Thériault, J. M., R. Rasmussen, K. Ikeda, and S. Landolt, 2012: Dependence of Snow Gauge
750 Collection Efficiency on Snowflake Characteristics. *J. Appl. Meteor. Climatol.*, **51**, 745–762,
751 <https://doi.org/10.1175/JAMC-D-11-0116.1>.

752 Trenberth, K. E., J. T. Fasullo, and J. Kiehl, 2009: Earth's Global Energy Budget. *Bull. Amer.*
753 *Meteor. Soc.*, **90**, 311–324, <https://doi.org/10.1175/2008BAMS2634.1>.

754 Uijlenhoet, R. 2001: Raindrop size distributions and radar reflectivity-rain rate relationships
755 for radar hydrology, *Hydrol. Earth Sys. Sci.*, **5**, 615–627. [https://doi.org/10.5194/hess-5-615-](https://doi.org/10.5194/hess-5-615-2001)
756 2001

757 Uijlenhoet, R., M. Steiner, and J. A. Smith, 2003: Variability of Raindrop Size Distributions
758 in a Squall Line and Implications for Radar Rainfall Estimation. *J. Hydrometeor.*, **4**, 43–61,
759 [https://doi.org/10.1175/1525-7541\(2003\)004<0043:VORSDI>2.0.CO;2](https://doi.org/10.1175/1525-7541(2003)004<0043:VORSDI>2.0.CO;2).

760 Vicente-Serrano, S. M., S. Beguería, and J. I. López-Moreno, 2010: A Multiscalar Drought
761 Index Sensitive to Global Warming: The Standardized Precipitation Evapotranspiration
762 Index. *J. Climate*, **23**, 1696–1718, <https://doi.org/10.1175/2009JCLI2909.1>.

763 Villarini, G., P. V. Mandapaka, W. F. Krajewski, and R. J. Moore, 2008: Rainfall and
764 sampling uncertainties: A rain gauge perspective, *J. Geophys. Res.*, **113**, D11102,
765 doi:10.1029/2007JD009214.

766 Wentz, F.J., D. Draper, 2016: On-Orbit Absolute Calibration of the Global Precipitation
767 Measurement Microwave Imager. *J. Atmos. Oceanic Technol.*, **33**, 1393–1412.
768 doi:10.1175/JTECH-D-15-0212.1

769 Whiton, R. C., P. L. Smith, S. G. Bigler, K. E. Wilk, and A. C. Harbuck, 1998a: History of
770 Operational Use of Weather Radar by U.S. Weather Services. Part I: The Pre-NEXRAD Era.
771 *Wea. Forecasting*, **13**, 219–243, [https://doi.org/10.1175/1520-](https://doi.org/10.1175/1520-0434(1998)013<0219:HOOUOW>2.0.CO;2)
772 0434(1998)013<0219:HOOUOW>2.0.CO;2.

773 Whiton, R. C., P. L. Smith, S. G. Bigler, K. E. Wilk, and A. C. Harbuck, 1998b: History of
774 Operational Use of Weather Radar by U.S. Weather Services. Part II: Development of
775 Operational Doppler Weather Radars. *Wea. Forecasting*, **13**, 244–252,
776 [https://doi.org/10.1175/1520-0434\(1998\)013<0244:HOOUOW>2.0.CO;2](https://doi.org/10.1175/1520-0434(1998)013<0244:HOOUOW>2.0.CO;2).

777 Witze A, 2018: The Quest to Conquer the Space Junk Problem. *Nature* **561**, 7721, 24–26.
778 <https://doi.org/10.1038/d41586-018-06170-1>

779 Wu, Y., and F. Weng, 2011: Detection and correction of AMSR-E radio-frequency
780 interference. *Acta Meteorol Sin* **25**, 669–681. <https://doi.org/10.1007/s13351-011-0510-0>

781 Zhang, J., and Coauthors, 2011: National Mosaic and Multi-sensor QPE (NMQ) System:
782 Description, Results, and Future Plans. *Bull. Amer. Meteor. Soc.*, **92**, 1321-1338.
783 <https://doi.org/10.1175/2011BAMS-D-11-00047.1>
784 Zhang, J., and Coauthors, 2016: Multi-Radar Multi-Sensor (MRMS) Quantitative
785 Precipitation Estimation: Initial Operating Capabilities. *Bull. Amer. Meteor. Soc.*, **97**, 621–
786 638, <https://doi.org/10.1175/BAMS-D-14-00174.1>.
787

788

789 **Sidebar 1:**

790 **Precipitation Characteristics**

791 The requirements for observing precipitation are driven by the very specific scale and
792 characteristics that precipitation exhibits, creating a challenging statistical problem.

793

794 At the micro-physical scale water is the only element that co-exists in all three phases,
795 namely vapour, liquid, and solid, a situation that is common in many precipitation systems.
796 Liquid-phase water starts with the formation of water droplets (about 10 μm), usually on
797 cloud condensation nuclei (c.0.1 μm), through the growth of cloud droplets, to precipitation-
798 sized particles (c.100 μm , up to 4-5 mm; Ma et al. 2019). Smaller droplets are spherical, but
799 large droplets become flatter or even umbrella-shaped due to air resistance prior to breakup.
800 Pristine ice-phase water particles have similar growth, except physical aggregation of
801 particles and interactions with liquid (riming) also occur. The resulting icy particles exhibit a
802 vast range of shapes and sizes, with significant implications for the retrieval and estimation of
803 (frozen) precipitation.

804

805 At the precipitation system scale the mechanisms driving the microphysical processes that
806 form clouds and falling precipitation result in variations in precipitation that range from a few
807 metres to 1000 km or more, and from a few seconds through to days, weeks, and longer
808 (Trenberth et al. 2009). Thus, the observation of precipitation is very much affected by
809 interaction between the time/space scales of the rain being observed and the
810 resolution/sampling of the observing system (Luini and Capsoni 2012).

811

812 The precipitation statistics in space/time are unusual in that the normal/modal value is zero:
813 for most of the time, and for the majority of the globe it is not raining/snowing. Furthermore,
814 when precipitation does occur, it is heavily skewed towards light precipitation intensities,
815 while the accumulation of precipitation (being a function of occurrence \times intensity) is more
816 log-normally distributed (see Figure SB1). As instantaneous samples are accumulated over
817 time and space, the distribution shifts towards a more normal distribution. This complicates
818 any statistical evaluation and requires extreme care when analysing or evaluating
819 precipitation data sets. Specifically, the distribution of precipitation intensities is very much
820 dependent upon the spatial and temporal scales being considered (Luini and Capsoni 2012),
821 such that observing a precipitation system at the same time with sensors with different spatial
822 resolution will yield different results. Similarly, comparing instantaneous precipitation with
823 precipitation accumulated over a few minutes, days, or months will reveal very different
824 characteristics. The practical implication is that instantaneous point measurements cannot be
825 directly compared with those collected over an area and/or over time. This issue in
826 compounded by the fact that precipitation events tend to last for periods ranging from a few
827 minutes to hours.

828

829
830
831

Table 1: Characteristics of present-day LEO and GEO satellites and their observational capabilities.

| | Orbit | LEO¹ | GEO² |
|---------------|--|--|--|
| Band | Characteristics | 400-800 km altitude orbits c.14-16 orbits/day Polar orbiting Sun-synchronous (up to 2 overpasses/day), or Low inclination precessing orbits | c.36,000 km altitude orbits Geosynchronous orbit – satellite remains stationary relative to sub-satellite point. |
| Vis/IR | Cloud top properties Reflection, emission (T) Texture & particle sizes | Multi-spectral Orbital swaths <1 m to 1 km | Multi-spectral Frequent/regular samples over sectors or full disk coverage <1-4 km footprints at sub-satellite point |
| PMW | Hydrometeor column Liquid, ice and water vapour | Multi-channel Orbital swath c.5 – 70 km footprints | <i>Not possible at present</i> <i>Several feasibility studies</i> |
| AMW | Vertical profiles of hydrometeors Backscatter Liquid, ice | Single/dual frequency (13.6/35/94 GHz) Single beam (CloudSat with 1.4/5.4 km footprints) or narrow swath (DPR 245 km swath and 5.4x5.4 km footprints) | <i>Not possible at present</i> <i>Some feasibility studies</i> |

832
833
834
835
836
837
838
839
840
841
842

¹ LEO: Vis/IR observations provided by a large group of sensors ranging from land surface monitoring missions (e.g. Landsat) through to meteorological missions (e.g. AVHRR) with resolutions typically matched to user requirements. PMW channels used for the retrieval of geophysical and meteorological parameters, including precipitation.

² GEO: constellation of GEO satellites provides global coverage with frequent/regular observations, disseminated at a nominal 3 hourly interval, but with sensors typically providing operational 10-15 min. data collection, and rapid scans <1 minute.

843 Table 2: Microwave sensors contributing to the GPM precipitation constellation. The
 844 current precipitation constellation missions are highlighted in bold. (**retrieval*
 845 *resolution is that of the NASA GPROF scheme*).
 846

| Satellite | Agency | Sensor number | | Channels | Retrieval resolution* |
|-------------------------------|----------------------|---------------|-----------|-------------------------|--------------------------|
| AMW instruments | | | | | |
| GPM | NASA/JAXA | DPR | x1 | 13.6/35.5 GHz | 5.4 x 5.4 km |
| <i>TRMM</i> | <i>NASA/JAXA</i> | <i>PR</i> | | <i>13.6 GHz</i> | <i>4.3 x 4.3 km</i> |
| PMW imagers | | | | | |
| GPM | NASA/JAXA | GMI | x1 | 10.7-183.31 GHz | 10.9 x 18.1 km* |
| DMSP F16,17,18,19 | US DoD | SSMIS | x3 | 19.35-183.31 GHz | 45 x 74 km* |
| GCOM-W1 | JAXA | AMSR2 | x1 | 6.7-89.0 GHz | 14 x 22 km* |
| <i>TRMM</i> | <i>NASA/JAXA</i> | <i>TMI</i> | | <i>10.7-89.0 GHz</i> | <i>20.9 x 34.6 km*</i> |
| PMW sounders | | | | | |
| NOAA-18,19 METOP-A,B,C | NOAA/EUMETSAT | MHS | x3 | 89.0-183.31 GHz | 17.12 x 21.64 km* |
| NPP, NOAA-20 | NOAA | ATMS | x2 | 23.0-183.31 GHz | 16.51 x 16.22 km* |
| MeghaTropiques | ISRO/CNES | SAPHIR | x1 | 183.31 GHz (x6) | 7.34 x 7.27 km |

847

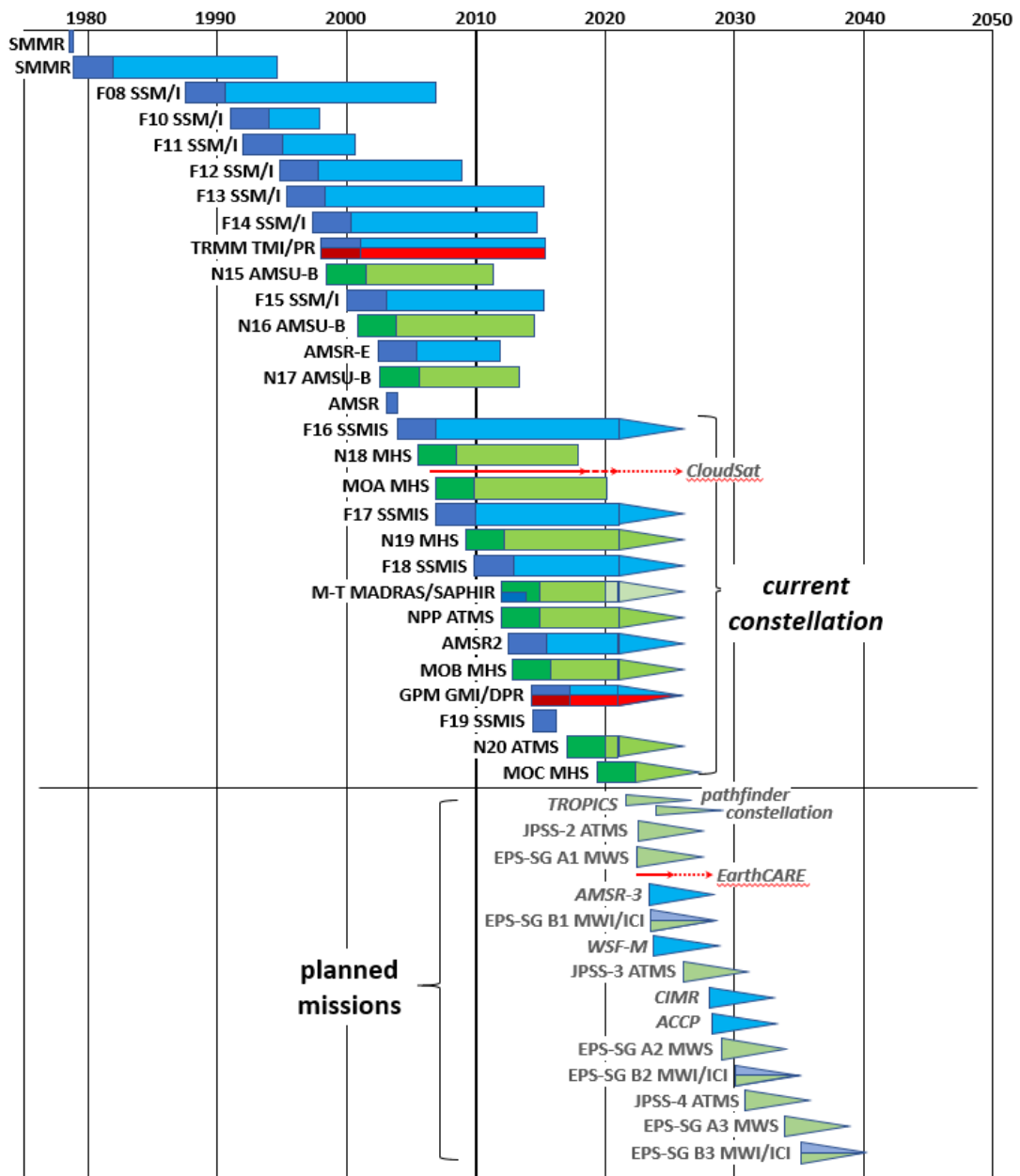
848

849

850 Table 3: Current GEO VIS/IR sensors: those that actively contribute to the global 30-
851 minute 4 km IR imagery are highlighted in bold. *(All of these provide multi-channel*
852 *VIS/IR observations with temporal sampling of 15 minutes or better, and < 1km / 4km*
853 *for VIS/IR at sub-satellite point).*
854

| Satellite | Agency | Sensor | Longitude | Channels/number | Sub-satellite resolution |
|----------------------------|-----------------|---------------|----------------|-------------------|--------------------------|
| GOES-13 (Storage) | NOAA | IMAGER | 60°W | VIS/IR x5 | 1 km / 4 km |
| GOES-14 (backup) | NOAA | IMAGER | 105°W | VIS/IR x5 | 1 km / 4 km |
| GOES-15 (West backup) | NOAA | IMAGER | 128°W | VIS/IR x5 | 1 km / 4 km |
| GOES-16 (GOES-East) | NOAA | ABI | 75.2°W | VIS/IR x16 | 0.5 km / 2 km |
| GOES-17 (GOES-West) | NOAA | ABI | 137.2°W | VIS/IR x16 | 0.5 km / 2 km |
| Meteosat-8 (IODC) | EUMETSAT | SEVIRI | 41.5°E | VIS/IR x12 | 1 km / 3 km |
| Meteosat-9 (rapid scan) | EUMETSAT | SEVIRI | 3.5°E | VIS/IR x12 | 1 km / 3 km |
| Meteosat-10 (rapid scan) | EUMETSAT | SEVIRI | 9.5°E | VIS/IR x12 | 1 km / 3 km |
| Meteosat-11 | EUMETSAT | SEVIRI | 0° | VIS/IR x12 | 1 km / 3 km |
| Himawari-8 | JMA | AHI | 140.7°E | VIS/IR x16 | 0.5 km / 2 km |
| Himawari-9 (standby) | JMA | AHI | 140.7°E | VIS/IR x16 | 0.5 km / 2 km |

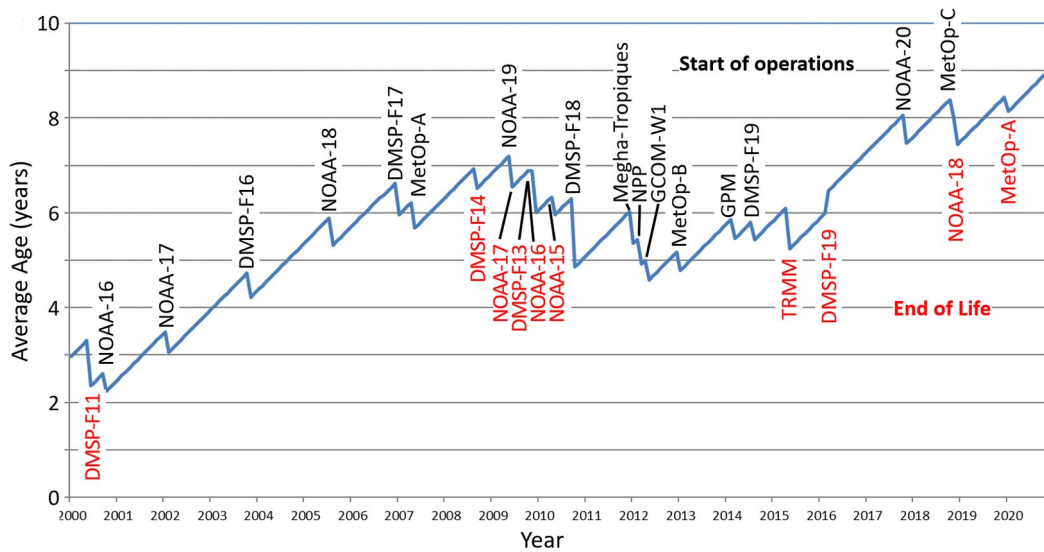
855



857

858 Figure 1: Timeline of PMW satellites and sensors providing analysis-ready data. The wide
 859 bars and arrows indicate swath-based or nadir-only observations respectively. Blue bars
 860 represent imaging/conical scanning radiometers, green bars represent sounding/cross-track
 861 radiometers and red bars indicate AMW (radar) sensors. Triangles indicate those sensors that
 862 currently provide data (as of 2021-02-09) and may continue to do so, together with future
 863 missions. (Data source: based upon World Meteorological Office (WMO) Observing Systems
 864 Capability Analysis and Review Tool (OSCAR) database and EUMETSAT)

865



866

867

Figure 2: Mean age of the PMW satellites up to 1st January 2021. From 2005-2016 the mean age was around 5-7 years, but now currently exceeds 9 years. Note that the constellation becomes younger both with a new launch and if a long-term mission reaches its end of life.

868

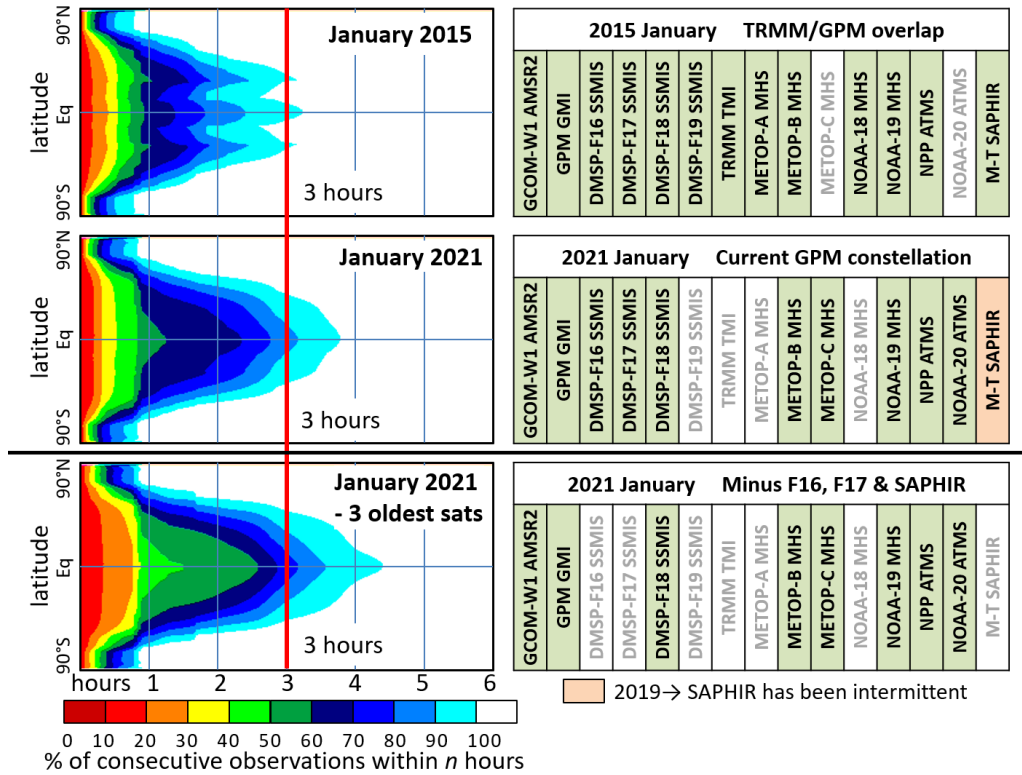
869

870

871

872

873



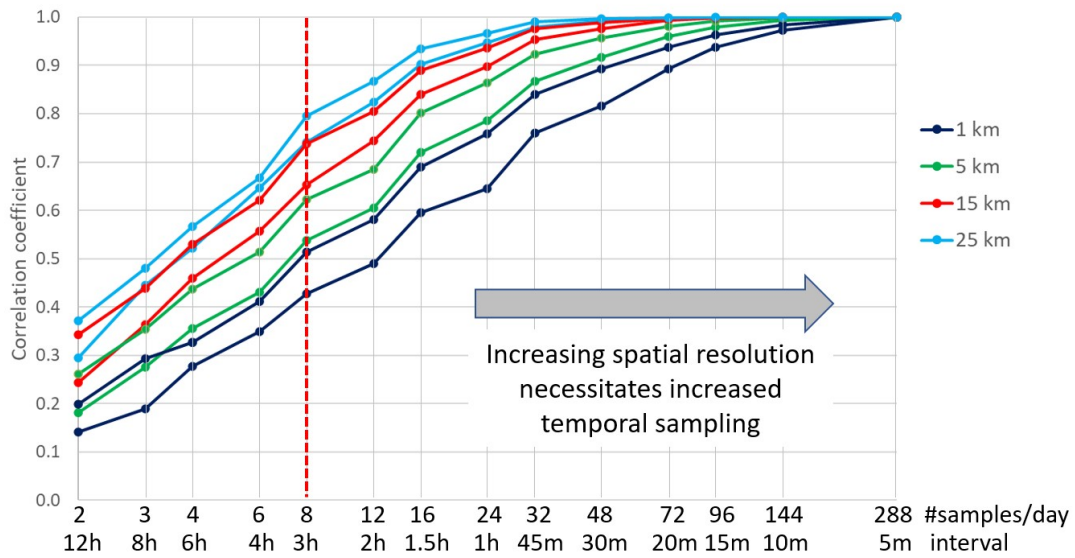
875

876

877 Figure 3: Comparison of the revisit times by latitude for three selected dates: the baseline
 878 sampling of the GPM mission is shown in the top row for January 2015, while the current
 879 sampling is shown in the middle row for January 2021. The bottom row shows a possible
 880 scenario if data from the three oldest sensors (SSMIS F16 and F17, and SAPHIR) are not
 881 included. The red vertical line represents the widely accepted 3-hour minimum revisit time
 882 necessary to adequately capture the accumulation of precipitation at daily, 0.25° scales.
 883 While the 3-hour revisit time was attained more than 90% of the time in January 2015, the
 884 reduction in the constellation numbers has reduced this to about 80% in January 2021.

885

886



887

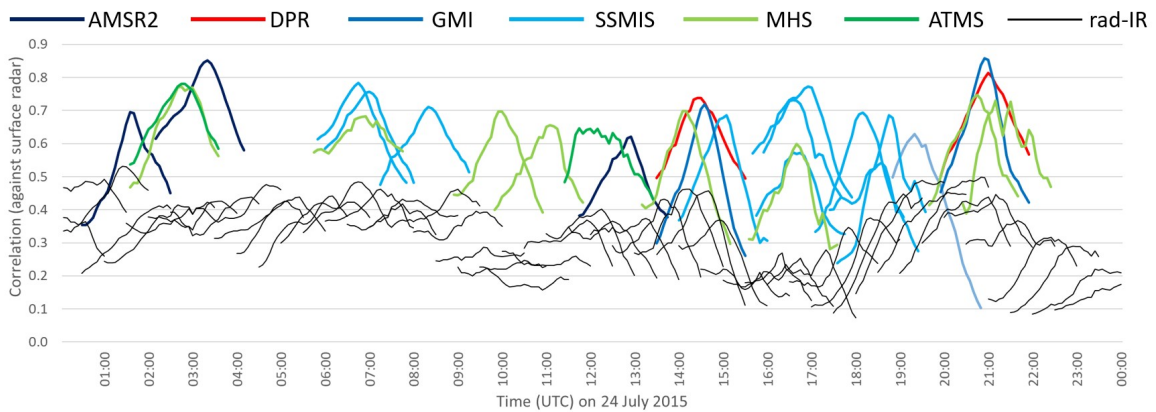
888

889 Figure 4: correlation between temporally sub-sampled 5-minute 1-km radar data and the daily
890 total (accumulating all 5-min. samples) for two 300x300 km areas (for each resolution) over
891 the central UK during 2019. Despite the different relationships within each resolution
892 category due to regional variations in precipitation characteristics, the general trend is that
893 finer spatial resolutions require more samples. Note that for the nominal 3-hourly sampling
894 (8 samples/day) the correlation is only between 0.4-0.5 at 1 km resolution, and no better than
895 0.8 at 25 km resolution.

896

897

898



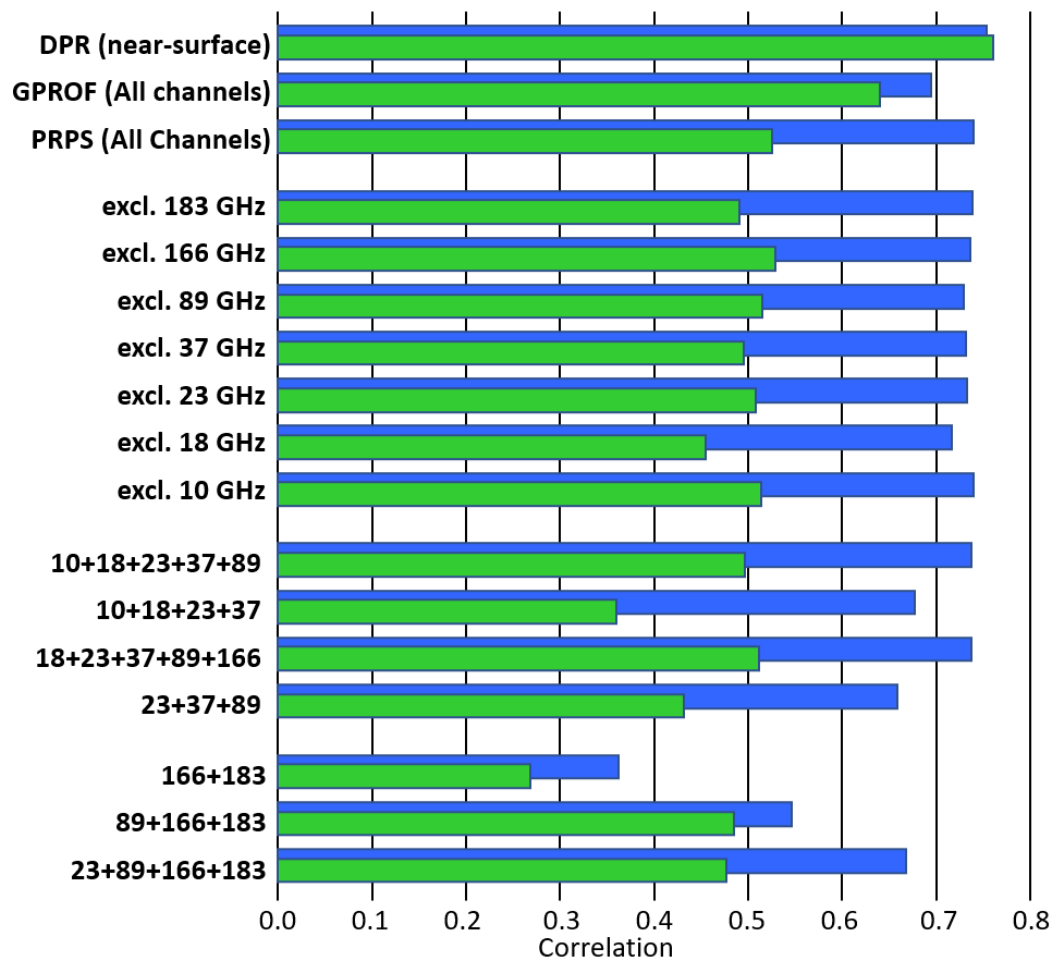
899

900 Figure 5: Correlation of satellite precipitation retrievals from IR, passive, and AMW sensors
901 against surface radar for 24 July 2015 over the central UK. Each line segment covers a
902 window over which the satellite estimate is compared with radar data up to ± 1 hour centred
903 on the observation time of the satellite sensor. The microwave measurements generally have
904 a good correlation at overpass time, but this falls quite quickly on either side of the
905 observation time. The estimates derived from the radar-calibrated 30-minute IR data are
906 much poorer (rad-IR), as shown by the thin black lines.

907

908

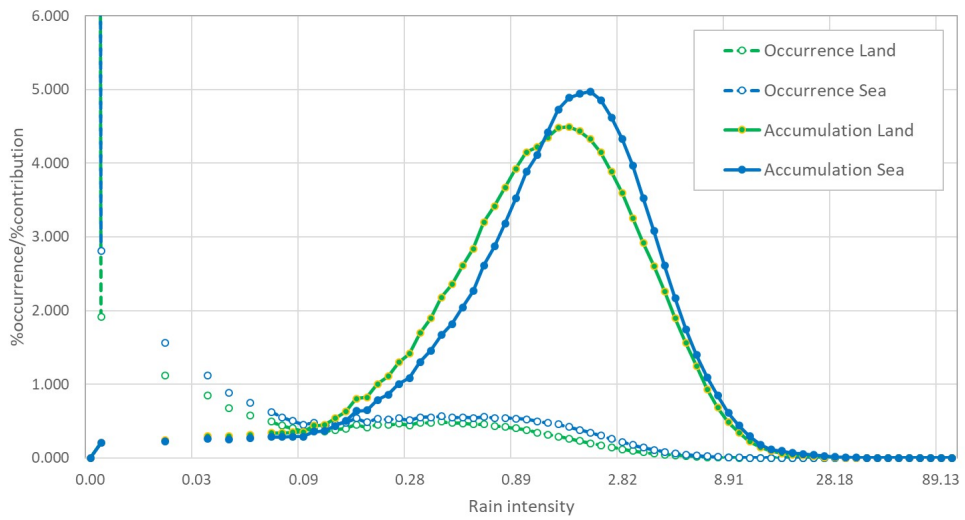
909



910

911 Figure 6: Scenarios used to study the effects of channel loss and channel combinations, based
 912 upon instantaneous PRPS retrievals from the 13-channel, 7-frequency GMI sensor, compared
 913 with surface radar data over the United Kingdom for 2017. The blue bars are for over ocean
 914 retrievals, while the green bars are for over land. The top three retrievals (DPR, GPROF and
 915 PRPS, where the last two are computed from GMI) can be used as benchmarks. The
 916 exclusion of a single channel has relatively little effect, except for the 18 GHz primarily over
 917 land. Generally, the more channels that are available, the better the retrieval as seen in the
 918 multi-frequency 10-89 or 18-166 GHz retrieval. A narrow frequency range results in poorer
 919 performance, particularly at high frequency channels, although the inclusion of a low
 920 frequency water vapour channel does significantly improve the performance over the ocean.

921



922
 923 Figure SB1: Distribution of the occurrence/contribution of precipitation by intensity based
 924 upon instantaneous surface radar data over the United Kingdom (2014-2019) at 15 km x 15
 925 km resolution. Note that the precipitation intensity is plotted on a log scale; the occurrence of
 926 precipitation is highly skewed towards zero.